

Self-energy effects and electron–phonon coupling in Fe–As superconductors

This article has been downloaded from IOPscience. Please scroll down to see the full text article.

2010 J. Phys.: Condens. Matter 22 115802

(<http://iopscience.iop.org/0953-8984/22/11/115802>)

View [the table of contents for this issue](#), or go to the [journal homepage](#) for more

Download details:

IP Address: 129.252.86.83

The article was downloaded on 30/05/2010 at 07:36

Please note that [terms and conditions apply](#).

Self-energy effects and electron–phonon coupling in Fe–As superconductors

K-Y Choi^{1,2}, P Lemmens¹, I Eremin^{3,4}, G Zwicknagl⁴, H Berger⁵,
G L Sun⁶, D L Sun⁶ and C T Lin⁶

¹ Institute for Condensed Matter Physics, TU Braunschweig, D-38106 Braunschweig, Germany

² Department of Physics, Chung-Ang University, Dongjak-Gu, Seoul 156-756, Republic of Korea

³ Max-Planck-Institut für Physik komplexer Systeme, D-01187 Dresden, Germany

⁴ Institut für Mathematische Physik, TU Braunschweig, D-38106 Braunschweig, Germany

⁵ Institute de Physique de la Matière Complexe, EPFL, CH-1015 Lausanne, Switzerland

⁶ Max-Planck-Institut für Festkörperforschung, Heisenbergstraße 1, D-70569 Stuttgart, Germany

Received 31 December 2009, in final form 14 February 2010

Published 5 March 2010

Online at stacks.iop.org/JPhysCM/22/115802

Abstract

Doping and temperature dependent studies of optical phonon modes in Fe-122 pnictides are performed using Raman scattering experiments and compared with model calculations to elucidate the role of electron–phonon and spin–phonon interaction in this family of compounds. The frequency and linewidth of the B_{1g} mode at around 210 cm^{-1} is highlighted as appreciable anomalies at the superconducting and spin density wave transitions are observed that strongly depend on composition. We give estimates of the electron–phonon coupling related to this renormalization and calculate the phonon self-energy on the basis of a four-band model comparing different symmetries of the order parameters. In addition, we observe a pronounced quasi-elastic Raman response for the undoped compound, suggesting persisting magnetic fluctuations in the spin density wave state.

(Some figures in this article are in colour only in the electronic version)

The recent discovery of superconductivity in iron arsenide compounds containing Fe_2As_2 layers with T_c higher than 50 K has stimulated enormous research activity [1–5]. This is largely due to the tantalizing possibility of finding a unified framework and description of a diverse range of unconventional superconducting materials.

Like for the high T_c cuprates, there is evidence for the importance of many-body effects. Inelastic neutron scattering (INS) measurements have uncovered a magnetic resonance peak for superconducting $\text{Ba}_{0.6}\text{K}_{0.4}\text{Fe}_2\text{As}_2$ [6]. The electron–phonon coupling is estimated to be a factor of five too weak to reproduce the observed transition temperature, even taking account of multiband effects [7]. Besides, the spin density wave (SDW) and the phase diagram with doping indicate an intimate relation between magnetism and superconductivity.

A combination of the specific band structure of the Fe pnictides [8] with antiferromagnetic correlations is proposed to lead to an s^\pm wave pairing state ($\Delta_{\mathbf{k}} = \frac{\Delta_0}{2}(\cos k_x + \cos k_y)$). The s^\pm -gap symmetry assumes a change of sign of the superconducting gap between electron and hole pockets and

the gap's magnitudes differing slightly on the hole and electron pockets. There is also a fictitious line of nodes between pockets which, however, does not cross the Fermi surface. This scenario is further supported by several theoretical works [9–11]. Although some spectroscopic experiments are consistent with s^\pm wave symmetry [3, 6, 12], there also exist data [13, 14] which cannot be easily fitted with a nodeless gap symmetry [15]. A nonuniversal gap symmetry can be resolved assuming a relatively large intraband Coulomb repulsion within each of the pockets. Depending on the model parameters, an extended s wave gap with a $\cos k_x/2 \cos k_y/2$ dependence and nodal lines crossing electron pockets centered around the M point [16, 17] or different symmetries like the d_{xy} wave ($\sin k_x \sin k_y$) or $d_{x^2-y^2}$ wave ($\cos k_x - \cos k_y$) symmetries [18, 19] can be obtained.

The prevailing trust in a magnetically mediated pairing mechanism with moderate electron–phonon coupling has been further justified by the observation of an inverse isotope effect on iron with $\alpha \sim -0.18$ in $\text{Ba}_{1-x}\text{K}_x\text{Fe}_2\text{As}_2$ [20, 21]. At the same time, Eschrig [22] asserted that an in-plane B_{1g} mode

might have a large electron–phonon coupling constant, which is more relevant to superconductivity than the averaged modes.

Raman spectroscopy is an experimental tool of choice for studying the strength of electron–phonon coupling [23–25]. In fact, earlier Raman works have investigated the SDW and superconducting properties of pnictides [26, 27, 29–31]. Still further combined experimental/theoretical studies of electron–phonon coupling are needed. In this paper, we provide spectroscopic information on the B_{1g} phonon renormalization upon entering into the superconducting phase. In particular, we address the electron–phonon coupling constant and calculate the evolution of the phonon self-energy for different gap symmetries.

For Raman scattering experiments, single crystals with dimensions of $3 \times 2 \times 0.2 \text{ mm}^3$ were used. The samples were grown by the flux growth method using solvents in zirconia crucibles under an argon atmosphere [28]. The superconducting transition temperatures of $T_c = 28 \text{ K}$ and $T_c = 32 \text{ K}$ for $\text{Sr}_{0.85}\text{K}_{0.15}\text{Fe}_2\text{As}_2$ and $\text{Ba}_{0.72}\text{K}_{0.28}\text{Fe}_2\text{As}_2$, respectively, were identified by transport and resistivity measurements. As a lattice reference we used the diamagnetic, isostructural compound FeAs_2 . The samples were kept in the vacuum of an optical cryostat equipped with a closed cycle refrigerator. Raman scattering experiments were performed using the excitation line $\lambda = 532 \text{ nm}$ (Nd:YAG solid-state laser) in a quasi-backscattering geometry. A laser power of 5 mW was focused to a 0.1 mm diameter spot on the surface of the single crystal. The scattered spectra were collected by a DILOR-XY triple spectrometer and a nitrogen cooled charge-coupled device detector.

Figure 1(a) shows the Raman response $\text{Im}\chi$ of the undoped SrFe_2As_2 for (xx) and (xy) polarizations at 290 K, which is corrected by the Bose thermal factor $[1 + n(\omega)] = [1 - \exp(-\hbar\omega/k_B T)]^{-1}$ from the measured Raman scattering intensity. At room temperature we observe a single peak at 203 cm^{-1} in the (xx) polarization. This is part of four symmetry-allowed modes: $\Gamma_{\text{Raman}} = A_{1g}(x^2 + y^2, z^2) + B_{1g}(x^2 - y^2) + 2E_g(xz, yz)$ [26, 27]. The 203 cm^{-1} mode is assigned to a B_{1g} mode and corresponds to a displacement of Fe atoms along the c axis.

The room temperature Raman response exhibits a structured background, which might be composed of a phonon density of states and weak electronic Raman scattering. To remove extrinsic effects, like defect scattering and contributions from the cryostat windows, $\text{Im}\chi(T = 290 \text{ K})$ is subtracted from $\text{Im}\chi(T)$. The resulting Raman response is plotted in figure 1(b) as a function of temperature. We observe a quasi-elastic scattering maximum, which is well described by a Lorentzian profile, $\text{Im}\chi \propto A\Gamma/(\omega^2 + \Gamma^2)$, where A is the scattering intensity and Γ is the full width at half-maximum. With decreasing temperature the scattering intensity grows steeply through T_s of the SDW and then shows a saturation for temperature below 130 K (see figure 1(c)). The full width at half-maximum tends to go to zero quasi-linearly upon cooling (see figure 1(d)). A central maximum can arise from the decay of a soft mode into acoustic modes or phonon density fluctuations in the presence of the structural phase transition. In our case, however, this does not give a dominant contribution

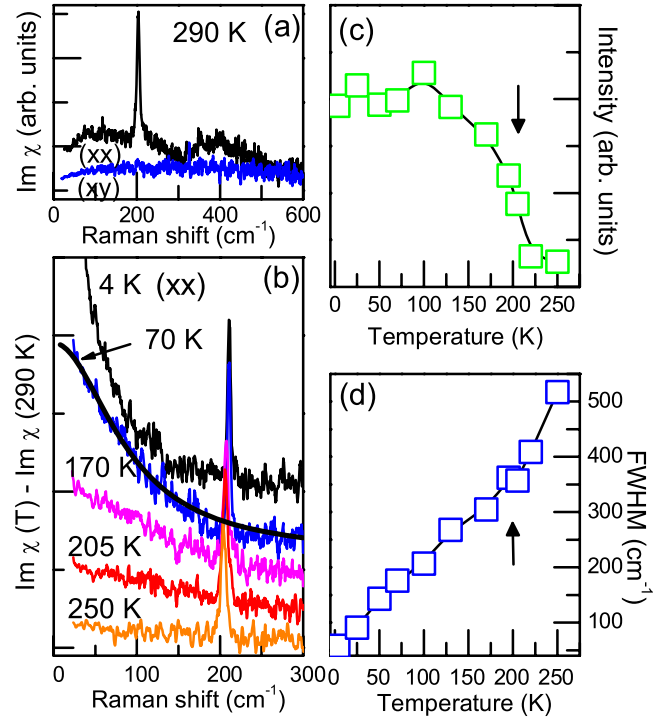


Figure 1. (a) Raman response $\text{Im}\chi$ of SrFe_2As_2 for (xx) and (xy) polarizations at 290 K. (b) Temperature dependence of the Raman response obtained by subtracting $\text{Im}\chi(290 \text{ K})$ from $\text{Im}\chi$. The solid line is a fit to a Lorentzian profile. (c) Temperature dependence of the scattering intensity. (d) Temperature dependence of the full width at half-maximum.

because the structural phase transition is of first order [28]. Actually, the intensity of the elastic maximum does not diverge at T_s . Instead, it looks similar to the temperature dependence of the elastic neutron scattering intensity at the AF superlattice reflection [32]. Thus, it is ascribed to light scattering by low energy magnetic fluctuations. It should be noted that the Bose-corrected Raman scattering intensity, i.e. the imaginary part of the Raman response function, should vanish in the limit $\Delta\omega \rightarrow 0$ to fulfil causality [23]. This means that for energies below our window of observability ($\Delta\omega > 30 \text{ cm}^{-1}$) additional low energy intensity develops with decreasing temperatures. Similar Lorentzian-lineshaped fluctuations are observed, e.g. in low dimensional quantum spin systems due to pronounced energy density fluctuations [33]. Therefore it is tempting to attribute the quasi-elastic scattering and the linear dependence of its linewidth to strong magnetic fluctuations at low energies, i.e. to the proximity of the SDW state to a quantum phase transition [34, 35].

In the following we will focus on Raman scattering on optical phonons. In order to understand the evolution of the SDW state the temperature dependence of the 203 cm^{-1} B_{1g} mode was analyzed by using a Lorentzian profile. In figure 2 the results are summarized together with those for BaFe_2As_2 ($T_s = 138 \text{ K}$) and CaFe_2As_2 ($T_s = 173 \text{ K}$). We note that this mode is susceptible to any change of the Fe d states around the Fermi level.

The phonon frequency and linewidth show characteristic anomalies in the temperature dependence [36]. For all samples

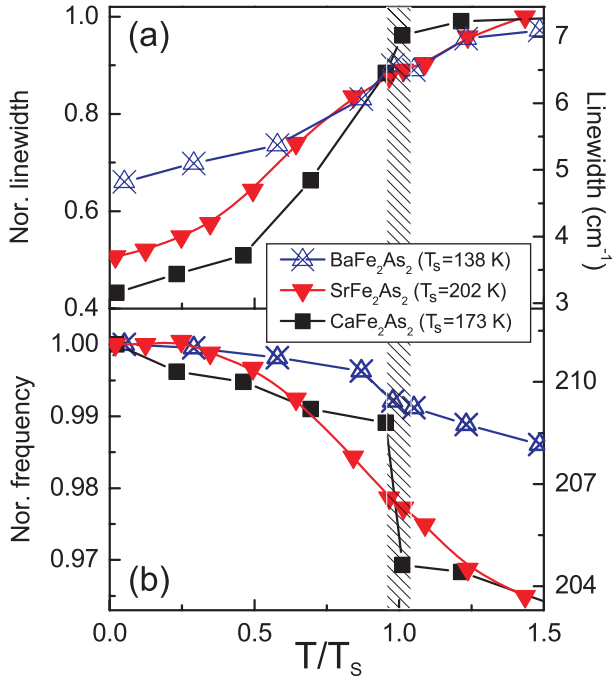


Figure 2. (a) Temperature dependence of the normalized linewidth and (b) peak position of the 203 cm⁻¹ mode on a reduced temperature scale, T/T_s . For comparison, SrFe₂As₂ ($T_s = 202$ K) is presented together with BaFe₂As₂ ($T_s = 138$ K) and CaFe₂As₂ ($T_s = 173$ K). The dashed, dotted, and solid lines are guides to the eyes.

we observe a jump of the phonon frequency and a narrowing of the linewidth below T_s . Similar phonon anomalies are observed in the A_{1g} mode [30], while the e_g phonon modes show a splitting related to its coupling to the structural distortions of the SDW [37]. Thus, we attribute the narrowing of the linewidth below T_s to a longer phonon lifetime in the SDW state and the depletion of electronic states on the Fermi surface. In contrast, we do not find a change of the scattering background that can be partially attributed to electronic Raman scattering. This suggests that the SDW gap is not fully opened on the Fermi surface.

This is consistent with the ARPES experiments [38] on the undoped pnictides where significant deviations from a complete nesting of the electron and hole Fermi surfaces have been found. Our results indicate that some of the non-nested Fermi surface portions will survive below T_s , producing a finite lifetime of phonons. In this regard the changes of the phonon self-energy below T_s will be less visible and depend on details of the band structure, i.e. stoichiometry. The observation that the phonon anomalies in CaFe₂As₂ are much more pronounced and abrupt than in SrFe₂As₂ and BaFe₂As₂ is consistent with a recent *ab initio* analysis [39] which found strongest nesting in CaFe₂As₂ followed by SrFe₂As₂. In addition the multiband character of the electronic structure of pnictides introduces an additional complexity. On the basis of purely symmetry considerations, it has been shown that the SDW ordering for the Fermi surface topology in pnictides will have little influence on some of the bands close to the Fermi energy even in the case of perfect nesting [40, 41]. This will further smooth the behavior of phonon self-energies across T_s .

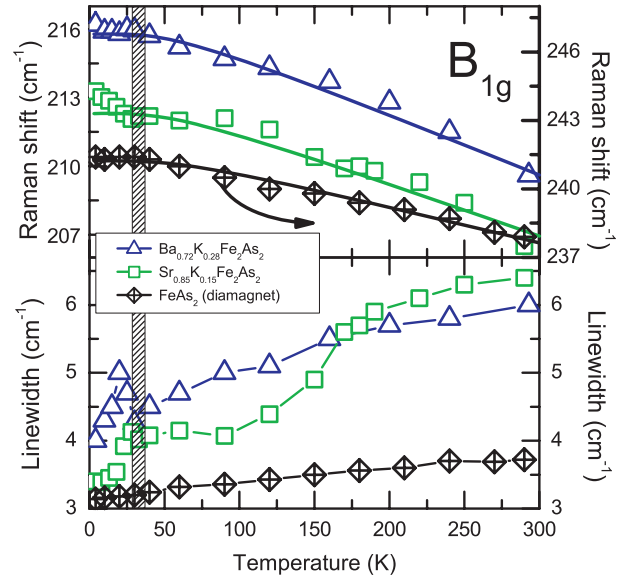


Figure 3. Temperature dependence of the peak position (upper panel) and linewidth (lower panel) of the B_{1g} mode for the Sr_{0.85}K_{0.15}Fe₂As₂ ($T_c = 28$ K) and Ba_{0.72}K_{0.28}Fe₂As₂ ($T_c = 32$ K) single crystals. For comparison, results for the diamagnetic, isostructural compound FeAs₂ are added. The solid lines are a fit to an anharmonic phonon decay process. The striped bar highlights the onset of the superconducting transition regime.

We now turn to the superconducting samples Sr_{0.85}K_{0.15}Fe₂As₂ and Ba_{0.72}K_{0.28}Fe₂As₂. The respective temperature dependence of the frequency and linewidth of the B_{1g} mode is shown in figure 3. In order to identify possible electron-phonon contributions, data for the diamagnetic isostructural compound FeAs₂ are presented as well. Its temperature dependence of the phonon frequency is well described in terms of simple phonon-phonon decay processes [42]:

$$\omega_{\text{ph}}(T) = \omega_0 + C[1 + 2/\exp(\hbar\omega_0/2k_B T) - 1]^{-1}$$

where ω_0 is the zero-temperature frequency of the B_{1g} mode and C corresponds to the anharmonic phonon decay processes. Also Ba_{0.72}K_{0.28}Fe₂As₂ follows largely the modeled anharmonic behavior. For Sr_{0.85}K_{0.15}Fe₂As₂ with a higher SDW transition temperature, however, we can find sizable deviations from the anharmonic profile. The frequency undergoes a small hardening by 1 cm⁻¹ at the superconducting T_c . This means that although the overall temperature dependence of the frequency is determined by the lattice anharmonicity, there are nonnegligible superconductivity-induced self-energy contributions. Interesting to note is that the SDW lead to an onset of anomalies in the phonon linewidth below 180 K for the Sr-based pnictide. For the Ba pnictide these anomalies for $T < 150$ K are much weaker. The overall decrease of linewidth with temperature is very pronounced and of similar magnitude to that for the undoped samples.

To analyze the effect of superconductivity on the renormalization of the B_{1g} phonons we employ the four-band model proposed previously [11] for the folded Brillouin zone. The unit cell contains two Fe and two As atoms and the band structure predicts a Fermi surface consisting of two hole (α)

pockets centered around the Γ point and two electron (β) pockets centered around the M point, respectively. A similar analysis has been previously performed for the buckling B_{1g} mode in cuprates within a single-band model [24].

Without taking into account vertex corrections, the renormalization of the optical phonons is determined by the Dyson equation:

$$D^{-1}(\mathbf{q}, \omega) = D_0^{-1}(\omega) - g_{\mathbf{q}}^2 \Pi(\mathbf{q}, \omega), \quad (1)$$

where $D_0(\omega) = \frac{2\omega_{\Gamma}}{\omega^2 - \omega_{\Gamma}^2 + i\delta}$ is the momentum independent bare phonon propagator and $g_{\mathbf{q}}$ is the corresponding electron-phonon coupling constant. The polarization operator is given by

$$\Pi(\mathbf{q}, \omega) = -i \int \text{Tr}[\tau_3 G(\mathbf{k} + \mathbf{q}, \Omega + \omega) \tau_3 G(\mathbf{k}, \Omega)] \frac{d^2k d\Omega}{(2\pi)^3}, \quad (2)$$

where $G(\mathbf{k}, \omega) = \frac{\omega I + \varepsilon_{\mathbf{k}} \tau_3 + \Delta_{\mathbf{k}} \tau_1}{\omega^2 - E_{\mathbf{k}}^2 + i\delta}$ is the propagator, $E_{\mathbf{k}}^2 = \varepsilon_{\mathbf{k}}^2 + \Delta_{\mathbf{k}}^2$ is the energy dispersion in the superconducting state, $\varepsilon_{\mathbf{k}}$ are the tight-binding energies for the α and β bands [11], and $\Delta_{\mathbf{k}}$ is a (momentum dependent) superconducting gap.

The various symmetries of the superconducting gaps will renormalize the polarization operator in the superconducting state differently. The main effect of superconductivity on the phonon self-energy at $\mathbf{q} = \mathbf{0}$ results from the change of the polarization operator of the two α bands. The latter, which are centered close to the Γ point, consequently couple rather strongly to the phonon dispersions around the center of the BZ. In figure 4(a) we show the changes of the real and imaginary parts of the polarization operators of the α bands for the extended s wave (s^{\pm}), and $d_{x^2-y^2}$ wave symmetries of the superconducting gap with respect to the normal state values. One can clearly see that the largest effect occurs for the extended s wave symmetry. The real part of the polarization operator in the superconducting state is larger for energies below $2\Delta_0$ than their normal state values and smaller for energies above $2\Delta_0$. This leads to a softening of the phonon frequencies with the corresponding sharpening of the phonon spectral function for those optical phonons whose energies are lower than $2\Delta_0$. The opposite behavior is found for $\omega_{\Gamma} > 2\Delta_0$. If the energy scales fit a nonmonotonic dependence of the phonon frequency, $\omega_q(T)$ may be observed as function of temperature. Overall, these results agree with the earlier ones [43]. An interesting remark here is that although similar behavior is found for d_{xy} wave (not shown) and $d_{x^2-y^2}$ wave symmetries it is much less pronounced due to the effectively smaller sizes of the gap at the Fermi surface of the α bands and the presence of the nodes. As a result the renormalization should be strongest for an extended s wave symmetry. Important to notice is that the behavior of the polarization operator is not affected by the inclusion of the higher harmonics in the extended s wave symmetry. The latter mostly affect the behavior of the gap around the M points and not at the Γ point where the coupling to the Raman-active phonons is present.

We also perform an analysis of the temperature dependence of the B_{1g} mode for temperatures below the

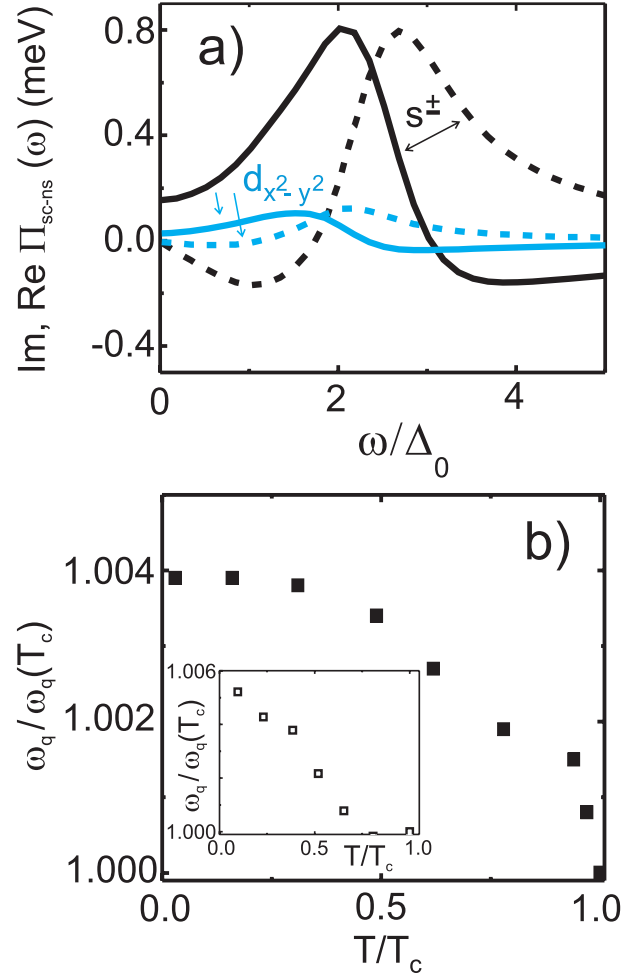


Figure 4. (a) Calculated difference of the polarization operator for the two α bands, $\Pi(\mathbf{q} \rightarrow 0, \omega)$ between the superconducting and normal states. The solid and dashed curves refer to the real and imaginary components, respectively. (b) Calculated normalized temperature dependent B_{1g} frequencies for temperatures below T_c . The inset shows the experimental data for $\text{Sr}_{0.85}\text{K}_{0.15}\text{Fe}_2\text{As}_2$ extracted from figure 3.

superconducting transition temperature assuming an extended s^{\pm} wave symmetry. The respective results are shown in figure 4(b). Using the previous estimates for the electron-phonon coupling strength of $g_{\mathbf{q}=\mathbf{0}} = 24.8$ meV and the bare $\hbar\omega_{B_{1g}} \approx 26.2$ meV in iron pnictides [44], we calculate the renormalization of the phonon frequency and find its hardening in the normal state at $T = 100$ K to 26.3 meV which corresponds to 210.4 cm^{-1} . Below T_c , $\text{Re } \Pi(\omega)$ further decreases at energies larger than $2\Delta_0 \approx 13.5$ meV which agrees well with the experimental data shown in the inset of figure 4(b). At the same time, we also find a broadening of the phonon mode below T_c (not shown) though experimentally our data show a quick switch of the broadening tendency into a sizable narrowing. Such change may occur only if $\hbar\omega_0 \sim 2\Delta_0$ or slightly smaller, which would yield anomalously large $2\Delta_0/k_B T_c$ ratios. One of the possible explanations could be microscopic coexistence of SDW and superconductivity or interband scattering effects which we leave for further studies. Evidence for coexistence, phase competition or separation on

different length scales has indeed been claimed [45]. These effects seem to depend in a critical way on the stoichiometry and therefore deserve further investigations.

Now we estimate the electron–phonon coupling strength. The linewidth of the isostructural compound FeAs₂ is given as 3–4 cm⁻¹ between 4 K and room temperature. Taking into account the linewidth of 3–7 cm⁻¹ and the superconductivity related narrowing of 1–2 cm⁻¹ in Ba_{0.72}K_{0.28}Fe₂As₂ and Sr_{0.85}K_{0.15}Fe₂As₂, the electron–phonon contribution does not exceed 2 cm⁻¹. The Allen equation provides a relation between the phonon linewidth, Γ , due to electron–phonon coupling and the phonon coupling constant [46]: $\Gamma = 2\pi\lambda_{B_{1g}}N(0)\omega^2$ where $\lambda_{B_{1g}}$ is the strength of the electron–B_{1g} coupling and $N(0)$ is the density of states (DOS) on the Fermi surface. For BaFe₂As₂, the total DOS at E_F is taken as $N(0) = 3.06 \text{ eV}^{-1}/\text{f.u.}$ [47]. If we assume that $N(0)$ remains constant for a small doping level, the electron–phonon constant is estimated to be $\lambda_{B_{1g}} \approx 0.02$.

We can also obtain the electron–phonon constant at the Brillouin zone center using the superconductivity-induced renormalization constant $\kappa = (\omega^{SC}/\omega^N) - 1 \approx 0.5\%$ [43]: $\lambda_{B_{1g}}^{\Gamma\text{-point}} = -\kappa \text{Re}[(\sin u)/u] \approx 0.01$, where $u \equiv \pi + 2i \cosh^{-1}(\omega^N/2\Delta)$. Both values are much smaller than the theoretically estimated total average value of $\lambda \approx 0.2$ [7]. Our results indicate that conventional electron–phonon coupling is weak for the B_{1g} phonon mode. As indicated by the inverse isotope coefficient, however, we cannot rule out the significance of unconventional electron–phonon coupling due to multiband effects.

To conclude, we have presented a Raman scattering study of undoped SrFe₂As₂ and superconducting Ba_{0.72}K_{0.28}Fe₂As₂ and Sr_{0.85}K_{0.15}Fe₂As₂ as a function of temperature. We observe a superconductivity-induced self-energy effect of the B_{1g} phonon mode and estimate the corresponding electron–phonon strength of $\lambda_{B_{1g}} \approx 0.02$.

Acknowledgments

This work was supported by the German Science Foundation DFG and the ESF program *Highly Frustrated Magnetism*. Work at the EPFL was supported by the Swiss NSF and by the NCCR MaNEP. KYC acknowledges financial support from the Alexander-von-Humboldt Foundation and the Korea Research Foundation Grant funded by the Korean Government (KRF-2008-313-C00247). We acknowledge important discussions with A V Chubukov, W Brenig, M Vavilov, B Keimer, R Valenti, and D Wulferding.

References

- [1] Kamihara Y, Watanabe T, Hirano M and Hosono H 2008 *J. Am. Chem. Soc.* **130** 3296
- [2] Takahashi H, Igawa K, Arii K, Kamihara Y, Hirano M and Hosono H 2008 *Nature* **453** 376
- [3] Chen X H, Wu T, Wu G, Liu R H, Chen H and Fang D F 2008 *Nature* **453** 761
- [4] Ren Z-A *et al* 2008 *Europhys. Lett.* **83** 17002
- [5] Rotter M, Tegel M and Johrendt D 2008 *Phys. Rev. Lett.* **101** 107006
- [6] Christianson A D *et al* 2008 *Nature* **456** 930
- [7] Boeri L, Dolgov O V and Golubov A A 2008 *Phys. Rev. Lett.* **101** 026403
- [8] Mazin I I, Singh D J, Johannes M D and Du M H 2008 *Phys. Rev. Lett.* **101** 057003
- [9] Kuroki K, Onari S, Arita R, Usui H, Tanaka Y, Kontani H and Aoki H 2008 *Phys. Rev. Lett.* **101** 087004
- [10] Bang Y and Choi H-Y 2008 *Phys. Rev. B* **78** 134523
- [11] Korshunov M M and Eremin I 2008 *Phys. Rev. B* **78** 140509(R)
- [12] Ding H *et al* 2008 *Europhys. Lett.* **83** 47001
- [13] Martin C *et al* 2009 *Phys. Rev. Lett.* **102** 247002
- [14] Fletcher J D, Serafin A, Malone L, Analytis J, Chu J-H, Erickson A S, Fisher I R and Carrington A 2009 *Phys. Rev. Lett.* **102** 147001
- [15] Vorontsov A B, Vavilov M G and Chubukov A V 2009 *Phys. Rev. B* **79** 140507(R)
- [16] Chubukov A V, Vavilov M G and Vorontsov A B 2009 *Phys. Rev. B* **80** 140515(R)
- [17] Maier T A, Graser S, Scalapino D J and Hirschfeld P J 2009 *Phys. Rev. B* **79** 224510
- [18] Moreo A, Daghofer M, Riera J A and Dagotto E 2009 *Phys. Rev. B* **79** 134502
- [19] Kuroki K, Usui H, Onari S, Arita R and Aoki H 2009 *Phys. Rev. B* **79** 224511
- [20] Shirage P M, Kihou K, Miyazawa K, Lee C-H, Kito H, Eisaki H, Tanaka Y and Iyo A 2009 *Phys. Rev. Lett.* **103** 257003
- [21] Choi H-Y, Yun J H, Bang Y and Lee H C 2009 *Phys. Rev. B* **80** 052505
- [22] Eschrig H 2008 arXiv:0804.0186 unpublished
- [23] Devereaux Th P and Hackl R 2007 *Rev. Mod. Phys.* **79** 175
- [24] Opel M, Hackl R, Devereaux T P, Virosztek A, Zawadowski A, Erb A, Walker E, Berger H and Forro L 1999 *Phys. Rev. B* **60** 9836
- [25] Donkov A, Korshunov M M, Eremin I, Lemmens P, Gnezdilov V, Chou F C and Lin C T 2008 *Phys. Rev. B* **77** 100504(R)
- [26] Litvinchuk A P, Hadjiev V G, Iliev M N, Lv B, Guloy A M and Chu C W 2008 *Phys. Rev. B* **78** 060503(R) and references therein
- [27] Choi K-Y, Wulferding D, Lemmens P, Ni N, Bud'ko S L and Canfield P C 2008 *Phys. Rev. B* **78** 212503 and references therein
- [28] Sun G L, Sun D L, Konuma M, Popovich P, Boris A, Peng J B, Choi K-Y, Lemmens P and Lin C T 2009 arXiv:0901.2728 and references therein
- [29] Granath M, Bielecki J, Holmlund J and Börjesson L 2009 *Phys. Rev. B* **79** 235103
- [30] Rahlenbeck M, Sun G L, Sun D L, Lin C T, Keimer B and Ulrich C 2009 *Phys. Rev. B* **80** 064509
- [31] Muschler B, Prestel W, Hackl R, Devereaux T P, Analytis J G, Chu J-H and Fisher I R 2009 *Phys. Rev. B* **80** 180510(R)
- [32] Zhao J *et al* 2008 *Phys. Rev. Lett.* **101** 167203
- [33] Lemmens P, Güntherodt G and Gros C 2003 *Phys. Rep.* **375** 1
Deisenhofer J and Lemmens P 2009 Optical techniques for systems with competing interactions *Frustrated Quantum Magnets* ed P Mendels and F Mila (New York: Springer) at press
- [34] Uhrig G S, Holt M, Oitmaa J, Sushkov O P and Singh R R P 2009 *Phys. Rev. B* **79** 092416
- [35] von Löhneysen H, Rosch A, Vojta M and Wölfle P 2007 *Rev. Mod. Phys.* **79** 1015
- [36] Gnezdilov V, Lemmens P, Zvyagin A A, Cheranovskii V O, Lamonova K, Pashkevich Yu G, Kremer R K and Berger H 2008 *Phys. Rev. B* **78** 184407 and references therein
- [37] Chauvière L, Gallais Y, Cazayous M, Sacuto A, Méasson M A, Colson D and Forget A 2009 *Phys. Rev. B* **80** 094504

- [38] Liu G *et al* 2009 arXiv:0904.0677
- [39] Zhang Y-Z, Kandpal H C, Opahle I, Jeschke H O and Valenti R 2009 *Phys. Rev. B* **80** 094530
- [40] Ran Y, Wang F, Zhai H, Vishwanath A and Lee D-H 2009 *Phys. Rev. B* **79** 014505
- [41] Eremin I and Chubukov A V 2010 *Phys. Rev. B* **81** 024511
- [42] Balkanski M, Wallis R F and Haro E 1983 *Phys. Rev. B* **28** 1928
- [43] Zeyher R and Zwirgmaier G 1990 *Z. Phys. B* **78** 175
- [44] Noffsinger J, Giustino F, Louie S G and Cohen M L 2009 *Phys. Rev. Lett.* **102** 147003
- [45] Chen H *et al* 2009 *Europhys. Lett.* **85** 17006
- Laplace Y, Bobroff J, Rullier-Albenque F, Colson D and Forget A 2009 arXiv:0907.3973v1
- Goko T *et al* 2009 *Phys. Rev. B* **80** 024508
- Park J T *et al* 2009 *Phys. Rev. Lett.* **102** 117006
- [46] Allen P B 1972 *Phys. Rev. B* **6** 2577
- [47] Singh D J 2008 *Phys. Rev. B* **78** 094511